BUTTERWORTH HEINEMANN

REVIEW

Computational fluid dynamics applied to internal gas-turbine blade cooling: a review

H. Iacovides and B. E. Launder
University of Manchester Institute of Science and Technology, Manchester, UK

This paper reviews current capabilities for predicting flow in the cooling passages and cavities of jet engines. Partly because of the need to enhance heat transfer coefficients, these flow domains entail complicated passage shapes where the flow is turbulent, strongly three-dimensional (3-D) and where flow separation and impingement, complicated by strong effects of rotation, pose severe challenges for the modeler. This flow complexity means that more elaborate models of turbulent transport are needed than in other areas of turbine flow analysis. The paper attempts to show that progress is being made, particularly in respect to the flow in serpentine blade-cooling passages. The first essential in modeling such flows is to adopt a low Reynolds number model for the sublayer region. The usual industrial practice of using wall functions cannot give a better than qualitative account of effects of rotation and curvature. It is shown that Rayleigh number effects can modify heat transfer coefficients in the cooling passages by at least 50%. The use of second-moment closure in the modeling is shown to be bringing marked improvements in the quality of predictions. Areas where, at present, more computational fluid dynamics (CFD) applications are encouraged are impingement cooling and pin-fin studies.

Introduction

Ask any gas turbine engineer about the impact of computational fluid dynamics (CFD) on gas-turbine design, and it is probable that the response will focus on the flow around the work input or output surfaces: the compressor and turbine blades. Perhaps, occasionally, one will be regaled with the progress and problems of predicting the very complex thermal and chemical development of flow through the combustion chamber. Almost never, however, will the focus of the response be on the prediction of flow *inside* the rotor or stator blades of the turbine or on the related flows in the turbine-disc cavities. These are flows that are acknowledged to be complex; however, because the main requirement is to determine just the surface heat transfer coefficient, that object is often perceived as being adequately and economically achieved by way of experimental correlations of generically similar flows coupled with rudimentary integral flow analysis.

To be fair, we must acknowledge that research sponsorship of CFD applied to internal cooling began at least a decade ago. It is, however, a measure of the complexity of the flows involved—from the both physical and computational points of view — that those 10 years have produced rather little in the form of well-validated, user-orientated software. However, although from outside, little may appear to be happening, much progress is being made both in the underlying scientific strategies of turbulence modeling, grid generation, and numerical solvers and in the application of these strategies to prototype flows. It is especially on the last of these that the present contribution focuses, dealing successively with the problems of rotation, both in cavities and tubing, U-bends, and the flow over ribs. Because the accurate modeling of turbulent transport underlies all these calculations, a brief overview of the essentials of second-moment closure with reference to internal cooling is given first in the following section.

Before that, some brief remarks are needed on areas *not* covered in this review. The area of pin-fin cooling does not yet appear to be one tackled by CFD: the nearest we found was a study by Lien (1993) of the flow around a finite length cylinder in a tube bank where heat transfer was not considered. That study ought, we believe, to encourage a start to be made on the many detailed and difficult problems in predicting heat transfer in the pin-fin configuration. Likewise, impingement cooling — at least studies directed explicitly at the special problems arising in the turbine-blade configuration — does not yet seem to have been attempted. A recent assessment by Craft et al. (1993) of the capabilities of four different turbulence models in predicting a single impinging jet on a flat plate should, likewise, lead to further more applied studies.

In the selection of examples in succeeding sections, the authors have drawn almost exclusively from work of the group at UMIST. This choice enables us to show the performance of a single modeling approach over a range of flows. Nevertheless, as

Address reprint requests to Prof. B. E. Launder, Mechanical Engineering Department, UMIST, Manchester, M60 1QK, UK.

Received 10 March 1995; accepted 28 July 1995

Int. J. Heat and Fluid Flow 16: 454–470, 1995

655 Avenue of the Americas, New York, NY 10010

0142-727X/95/$10.00
SSDI 0142-727X(95)00072-X

reference to other cited work makes clear, the CFD community as a whole is now tackling a diversity of internal cooling problems via CFD, and this effort should have an increasingly large impact on design strategy.

Turbulence modeling strategy

To begin with, we make a few general observations on the types of flow considered and their implications for the modeling path we have followed. First, the presence of strong Coriolis or centrifugal forces (perhaps both) will mean that there will be an intense near-wall secondary flow. A consequence of this is that any CFD scheme can only hope to capture the actual flow phenomena if the computations extend through the semi-viscous near-wall layer up to the wall itself. However economical, approaches for straddling the near-wall zone with "wall functions," predict much too little secondary flow with the result that the whole flow field may be quite unlike that actually arising. Second, streamline curvature is very considerable, and this, as is well known (Bradshaw 1973), makes the eddy-viscosity approach a highly dubious one for modeling turbulent transport, whatever the numerical attractions may be. These two "facts of life" have meant that our effort has been on modeling at "second-moment" level, at least in the core region of the flow where scales are relatively large, and effects of streamline curvature are greatest. There has, moreover, been a focus on refining low Reynolds number modeling partly because, as noted above, the interaction between the near-wall viscous sublayer and the secondary flow is so strong and partly because, in any event, it is this near-wall sublayer that is vitally important to mimic if the overall or, indeed, the *local* heat transfer coefficients are to be captured accurately.

It is instructive to *note* the exact transport equation for the Reynolds stress tensor, $u_i u_j$ expressed in Cartesian tensor notation:

$$\frac{D\overline{u_i u_j}}{Dt} = P_{ij} + \phi_{ij} - \varepsilon_{ij} + d_{ij} \tag{1}$$

where d_{ij}, ε_{ij}, and ϕ_{ij} denote, respectively, diffusive, dissipative, and nondispersive pressure interactions (causing, for example, intercomponent energy transfers) and where the generation tensor P_{ij} is given by

$$P_{ij} \equiv -\left(\overline{u_i u_k}\frac{\partial U_j}{\partial x_k} + \overline{u_i u_k}\frac{\partial U_i}{\partial x_k}\right) - 2\Omega_p\left(\varepsilon_{ipq}\overline{u_q u_j} + \varepsilon_{jpq}\overline{u_q u_i}\right)$$
$$- \frac{\overline{u_i \rho'}}{\rho}\left(\Omega_k X_k \Omega_j - \Omega_k \Omega_k X_j\right)$$
$$+ \frac{\overline{u_j \rho'}}{\rho}\left(\Omega_k X_k \Omega_i - \Omega_k \Omega_k X_i\right) \tag{2}$$

All the contributions to P_{ij} can be handled without further modeling. The interactions expressed by this tensor between the stress and strain fields are more subtle from those implied by the eddy-viscosity concept. For example, in a two-dimensional (2-D) flow, with primary strain $(\partial U_1/\partial X_2)$ but with a weak streamline curvature $(\partial U_2/\partial X_1)$, the generation rate of shear stress P_{12} is

$$-\left(\overline{u_2^2}\frac{\partial U_1}{\partial x_2} + \overline{u_1^2}\frac{\partial U_2}{\partial x_1}\right)$$

While $\partial U_1/\partial x_2$ may be one or two orders of magnitude greater than $\partial U_2/\partial x_1$, the fact that the streamwise normal stress component $(\overline{u_1^2})$ will be an order of magnitude greater than that normal to the wall $(\overline{u_2^2})$ means that the secondary strain associated with curvature has an unexpectedly large effect. In contrast, there is no such amplification of the effects of minor strains with the eddy-viscosity hypothesis, because each strain component is multiplied by the *same* scalar eddy-viscosity. Likewise, system rotation may readily be seen to produce a substantial effect on the Reynolds stresses. Consider a simple shear flow $(\partial U_1/\partial x_2)$ in a plane channel that is undergoing rotation about the x_3-axis (so-called orthogonal mode rotation). The generation of the shear stress is now

$$P_{12} = -\overline{u_2^2}\frac{\partial U_1}{\partial x_2} - 2\Omega\left(\overline{u_1^2} - \overline{u_2^2}\right)$$

where Ω is the angular rotation rate of the duct. Note that, while the first term changes sign with the mean velocity gradient (being positive on one side of the channel and negative on the other), the second is always negative provided that streamwise fluctuations, $\overline{u_1^2}$ exceed $\overline{u_2^2}$. Consequently, on the pressure side of the channel where $\partial U_1/\partial x_2$ is positive, the Coriolis and shear terms act in the same sense, and the magnitude of the shear stress is raised, while, on the suction side, they are in opposition producing a progressive reduction in shear stress levels as the importance of the Coriolis term increases. With an isotropic eddy-viscosity model, in contrast, because there is no Coriolis contribution in the turbulence energy budget, there is no predicted alteration in the turbulence structure.

There is a further effect of rotation on turbulence (the second and third lines of Equation 2), that can be important when temperature variations are large enough to cause substantial density fluctuations. It is analogous to the effects of gravity on turbulent mixing in the atmosphere; its influence will be greatest when the mean velocity is at right angles to the effective acceleration vector (the latter, in the present case, being radial). The steepest density gradients arise in the blade-cooling passages where the coolant passes largely radially. For this reason, the term's influence in current cooling configurations may be weak.

A few remarks, however brief, must be made about closure modeling of the unknown processes in Equation 1. First, it should, perhaps, be said that current applications do not use the most recent of closure strategies: most have employed linear eddy-viscosity models from the early 1970s or, occasionally, second-moment treatments of a similar vintage. Over the last few years, a new wave of modeling schemes has been proposed and applied with some success to a range of 2-D flows (e.g., Craft et al. 1993; Launder and Li 1994). These schemes have only just begun to find their way into blade or cavity cooling applications, but they *will* certainly be extensively used in this context in the next year or two, and, on their track record to date, it seems likely they will be successful. Here, however, attention is confined to the rudimentary treatments that *have* been adopted.

Table 1 Conventional coefficients

c_1	c_2	c_μ	c_s	$c_{\varepsilon 1}$	$c_{\varepsilon 2}$	$c_{\varepsilon 3}$	c_ℓ	σ_ε	σ_k
1.8	0.6	0.09	0.22	1.44	1.92	2.0	0.83	1.3	1.0

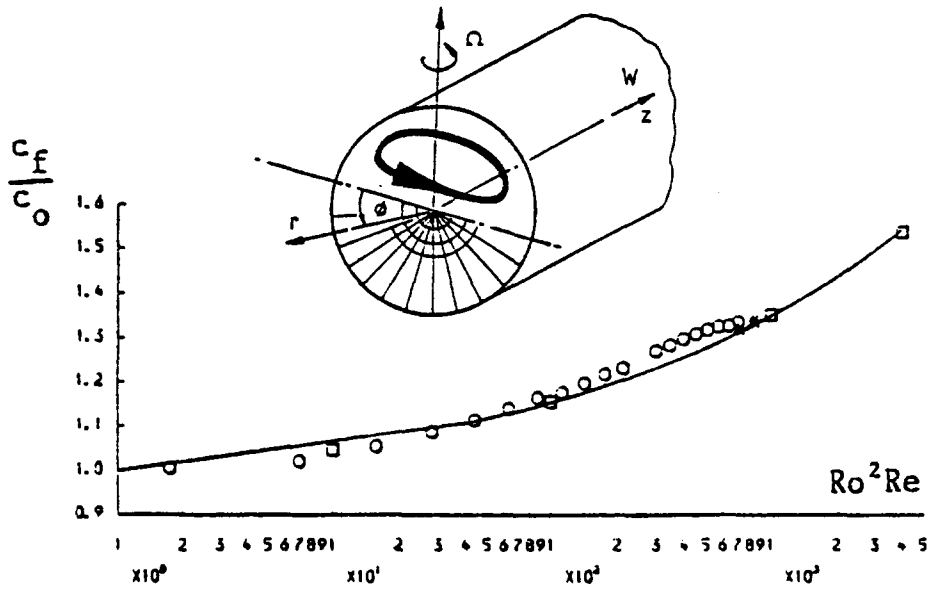

Figure 1 Average friction factor comparisons for fully developed flow in a rotating pipe; °□: ASM/mix. length: ∗: k-ε/mix. length: —: exp. correlation

Concerning the dissipation ε_{ij}, the customary route is to assume local isotropy and, thus

$$\varepsilon_{ij} = \frac{2}{3}\delta_{ij}\varepsilon \tag{3}$$

any weakness of this assumption being assumed to be accommodated in modeling ϕ_{ij}. Indeed, for this pressure–strain process, the conventional strategy has been to suppose,

$$\phi_{ij} = -c_1\frac{\varepsilon}{k}\left(\overline{u_iu_j} - \frac{2}{3}\delta_{ij}k\right) - c_2\left(P_{ij} - \frac{1}{3}\delta_{ij}P_{kk}\right) \tag{4}$$

where c_1 and c_2 are constant, and the repeated suffix (in P_{kk}) simply implies summation over all the normal-stress components. An objection to Equation 4 is that it is not invariant to rotation rate. There are various ways to remedy this (see, e.g. Fu et al. 1987), one of the simplest being to incorporate the convective transport term $c_{ij}(\equiv Du_iu_j/Dt)$ into the model

$$\phi_{ij} = -c_1\frac{\varepsilon}{k}\left(\overline{u_iu_j} - \frac{2}{3}\delta_{ij}k\right) - c_2\left(P_{ij} + c_{ij} - \frac{1}{3}\delta_{ij}(P_{kk} + c_{kk})\right) \tag{5}$$

A serious difficulty with either Equations 4 or 5 is that, in the vicinity of the wall, neither lead to sufficient damping of velocity fluctuations perpendicular to the surface. Consequently, "wall reflection" terms must be added (Launder et al. 1975) to avoid excessive levels of wall friction and heat transfer. However, such models were devised assuming the wall to be a single infinite plane surface (so that there is both an unambiguous direction normal to the wall and distance from the wall). Their application in the complex geometry of a blade-cooling passage entails both uncertainty and inaccuracy.

At best, simple gradient models have been adopted for stress transport

$$d_{ij} = \frac{\partial}{\partial x_k}\left[\left(\upsilon\delta_{k\ell} + c_s\frac{k}{\varepsilon}\overline{u_ku_\ell}\right)\frac{\partial u_iu_j}{\partial x_\ell}\right] \tag{6}$$

although the model is usually simplified from a *differential* to an *algebraic* second-moment (ASM) closure by way of Rodi's (1976) hypothesis:

$$(d_{ij} - c_{ij}) = (d_{kk} - c_{kk})\frac{\overline{u_iu_j}}{\overline{u_ku_k}}$$

$$= (P_{kk} - 2\varepsilon)\overline{u_iu_j}/2k \tag{7}$$

With this strategy, transport equations are solved for just the scalars k and ε. The former equation may be regarded as being handled exactly except for diffusive transport of k (which is usually represented by simple gradient transport with a turbulent Prandtl/Schmidt number close to unity). The quantity ε remains as an unknown and, with closures of the above type, it is obtained from essentially the same equation as that adopted in the

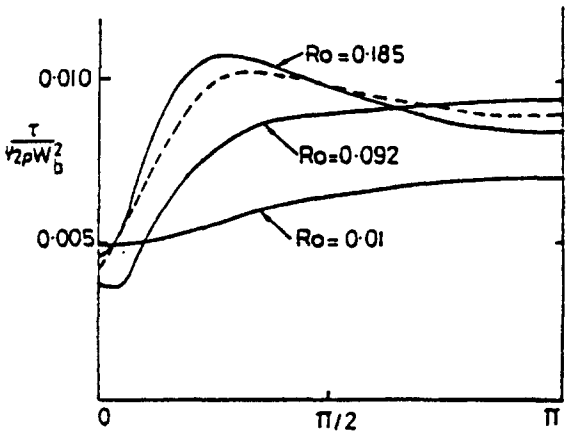

Figure 2 Local friction factor comparisons for fully developed flow in a straight rotating pipe; —: ASM/mix. length; – – –: k-ε/mix. length Ro = 0.185

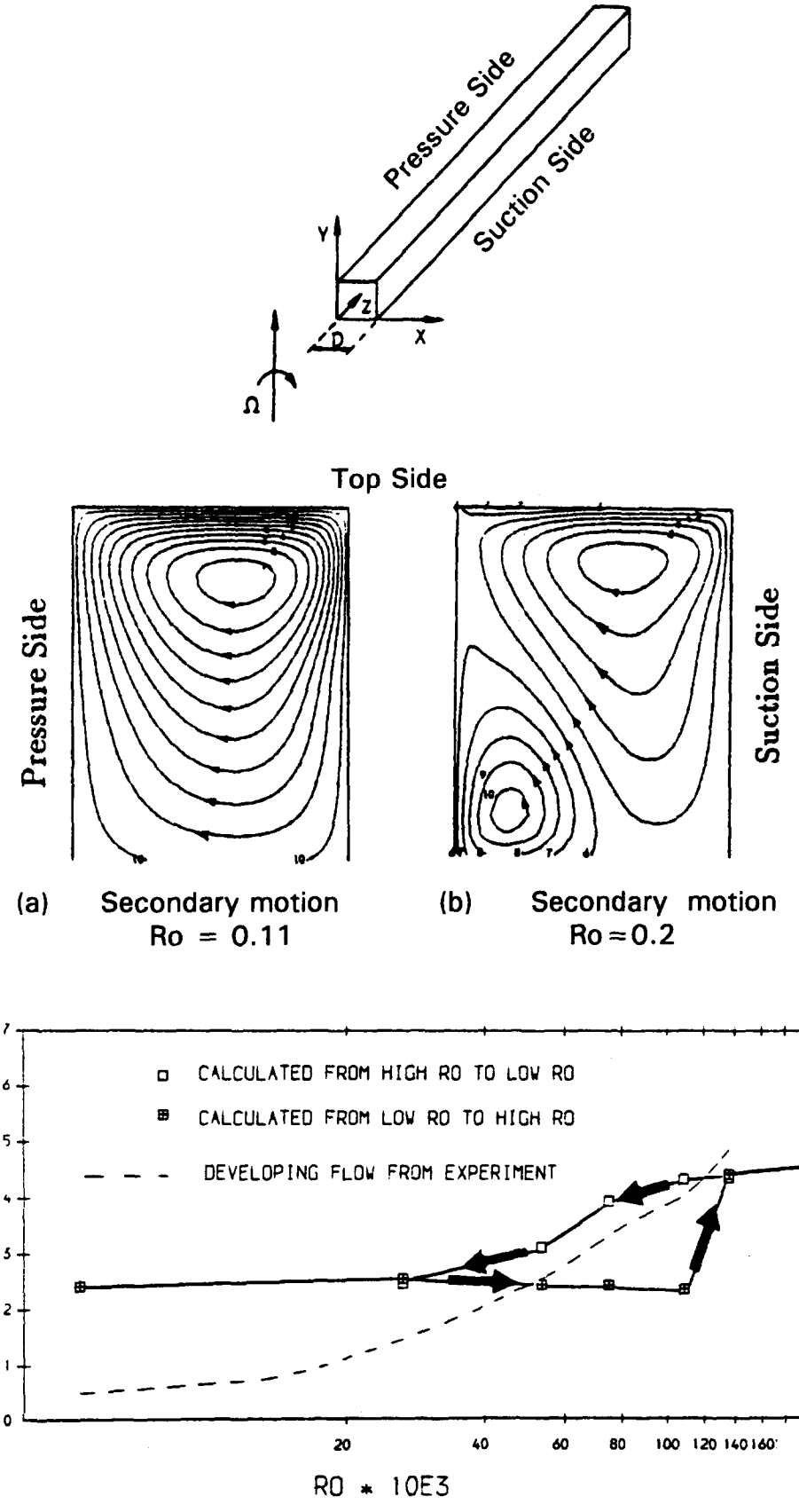

Figure 3 Transition from a two- to a four-vortex structure for fully developed flow through a rotating duct at Re = 33,000

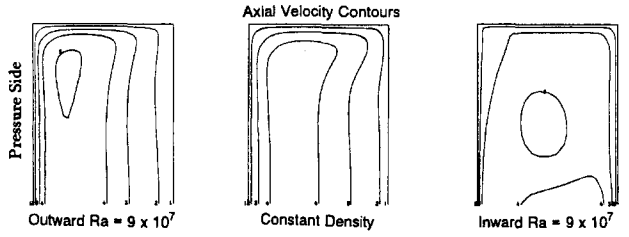

Figure 4 Effects of rotational buoyancy on fully developed flow through a rotating duct at Re = 33,000 and Ro = 0.11

k-ε linear eddy-viscosity model. The form conventionally used at UMIST is:

$$\frac{D\varepsilon}{Dt} = \frac{\partial}{\partial x_k}\left(\nu + \frac{\nu_t}{\sigma_\varepsilon}\right)\frac{\partial \varepsilon}{\partial x_k} + c_{\varepsilon 1}\frac{P_{kk}\varepsilon}{2k} - c_{\varepsilon 2}\frac{\varepsilon^2}{k} + c_l \frac{\ell}{\ell_e}\left(1 - \frac{\ell}{\ell_e}\right)\frac{\varepsilon^2}{k} + c_{\varepsilon 3}\nu\nu_t\left(\frac{\partial^2 U_i}{\partial x_i \partial x_k}\right)^2 \quad (8)$$

where ℓ is just the length scale $k^{3/2}/\varepsilon$, and ℓ_e is the equilibrium near-wall value $2.5y$, y being the wall distance. The conventionally adopted coefficients are listed in Table 1.

The first term on the second-line — the so-called Yap correction — is designed to prevent excessive near-wall length scales developing when turbulence energy generation rates are low there. As with the "wall-reflection" part of the pressure–strain model, it is not well designed for the complex shapes encountered in practical coolant passages, because the wall-normal distance appears.

Finally, it is as well to recall that usually the heat transfer coefficient is what the designer seeks. The effective thermal diffusivity is obtained by prescribing the turbulent Prandtl number. A uniform value of 0.9 is a simple and popular choice, although sometimes a more elaborate prescription near the wall is used in recognition of the peaking of thermal Prandtl number near the edge of the sublayer recorded in boundary layers (e.g., Kays and Moffat 1975). Alternatively, if the individual normal stresses are determined with reasonable accuracy, use of the generalized gradient–diffusion hypothesis arguably provides a more secure route for finding the heat flux, $\overline{u_i\theta}$

$$-\overline{u_i\theta} = c_\theta \overline{u_i u_j}\frac{k}{\varepsilon}\frac{\partial \Theta}{\partial x_j} \quad (9)$$

where the coefficient c_θ takes a value of approximately 0.30.

Although it is desirable to take account of the direct effects of force fields on the turbulent stresses, the effects of these forces in the *mean* momentum equations will usually be greater, because they will induce substantial modifications in the flow field. In the case of Coriolis forces, practical rotating ducts produce substantial x_3 variations in the axial velocity, which then leads to variations in the x_2-directed Coriolis force. These variations result in an appreciable secondary flow, especially within the viscosity-affected sublayer. A closely analogous effect arises with curved flows: an end wall (in the plane z = constant, say) reduces the tangential velocity U_θ and leads to a radially inward flow, because the radial pressure gradient (whose strength is largely determined by the motion further from the end wall) is larger than that required for purely circular motion. In turbulent flow, because the reduction of U_θ occurs predominantly across the viscous sublayer, the secondary motion again arises very close to the wall. Likewise, buoyant forces in the mean momentum equations again arise, predominantly, in the viscous layer, because it is across this sublayer that the density deviates most from the average value at a section. As in the case of buoyant effects on the fluctuating motion, the force acts radially.

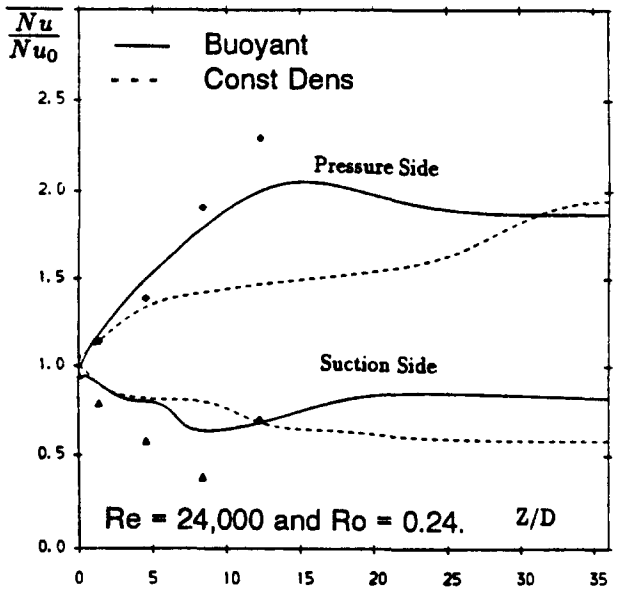

Figure 5 Nusselt number comparisons for developing flow in a rotating square duct; k-ε/one-eq computations

As far as modeling is concerned, the effect of these additional force fields in the momentum equations is double edged. On the one hand, they bring added complexity and, thus, increase the risk of getting the predicted flow pattern wrong. On the other hand, however, their appearance does not depend on the use of an elaborate turbulence model: the terms are present with an eddy-viscosity scheme just as plainly as with a second-moment closure. Indeed, it is solely this fact that enables eddy-viscosity schemes to be usefully applied to complex problems of blade cooling, especially because these source terms are strongest very close to the wall where the fluid undergoes (fairly) simple shearing. By the same token, it does mean that the near-wall viscosity-affected region must be treated with considerable respect. There the flow structure, in these cooling problems, is very different from that encountered in a simple, equilibrium shear flow — the type of flow used for developing "wall functions". For this reason, modeling approaches based on wall functions, while still very much the (announced) route adopted by industry (e.g. Tolpadi 1994), cannot provide a better than qualitative

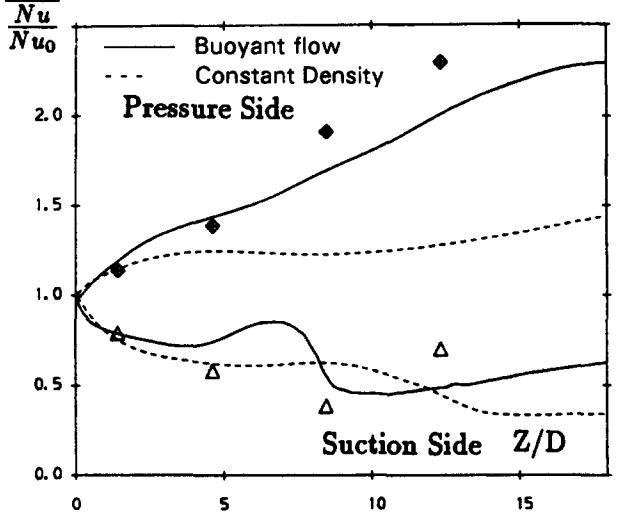

Figure 6 Nusselt number comparisons for developing flow in a rotating square duct; low-Re ASM computations

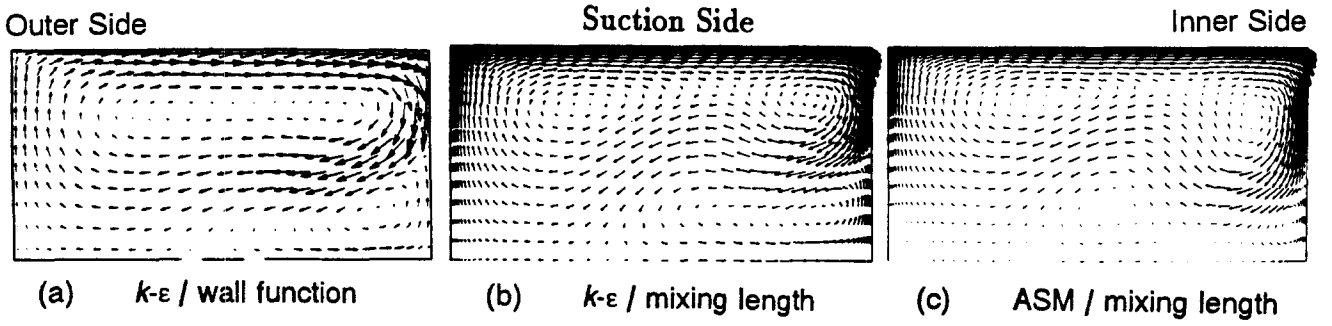

Figure 7 Secondary flow predictions for flow through a U-duct of curvature ratio, R_c/D, of 3.375 at $\theta = 135°$

indication of the effects of rotation, curvature, and strong heating on the flow pattern. Computational fluid dynamics can do better than that, and it is time to insist that it should do so.

Applications to blade cooling

We consider, in turn, the separate contributions of rotation and abrupt turning on the flow and thermal characteristics of passage flow. In practice, blade-cooling passages are shaped to fit in with the external profile of the blade, and consequently, their cross section is neither square nor circular. Experiments provided to help assess software performance or, more usually, to provide design correlations have, however, tended to adopt such simpler shapes. In making comparisons, the computer simulations have, likewise, considered the same simpler configurations. Where available, bends of square cross section have been considered here, because these are more difficult to predict than those of circular section. It is likely that actual cooling passages will exhibit a sensitivity to turbulence modeling intermediate between the two cases.

Flow in straight rotating ducts

Attention is given first to isothermal flows or, at least, to cases where buoyancy effects are negligible. Most numerical explorations have followed the original practice of Majumdar et al. (1977) and Majumdar and Spalding (1977) of matching the high Reynolds number k-ε model to wall functions. In fact, these workers found this approach led to satisfactory agreement for developing flow in a circular duct at low rotation rates, but agreement deteriorated as the rotation number, Ro ($\equiv \Omega D/U$), was increased. The same strategy has been retained by Howard et al. (1980), Sturgess and Datta (1987), Khodak et al. (1992), and Tolpadi (1994), although Howard and Khodak both introduced an empirical rotation correction tuned by reference to rotating channel flows of large aspect ratio where secondary flows were small. In application to square cavities, however, because of the strong secondary flow, the corrections had little effect, and only moderate agreement with measurements was achieved. We note, finally, that Younis (1993) also employed wall functions with a nonlinear k-ε model and, likewise, achieved only modest agreement with experiment. As asserted in the Turbulence modeling strategy section, it is *essential* to resolve the near-wall sublayer to secure close agreement with the measured behavior.

The first computations of rotating pipes that extended through the viscous layer were provided by Taylor et al. (1985) who followed the growing practice of that period, in other three-dimensional (3-D) flows, of interfacing the standard k-ε model in the turbulent part of the flow with Van Driest's (1956) form of the mixing-length hypothesis across the near-wall sublayer. De-

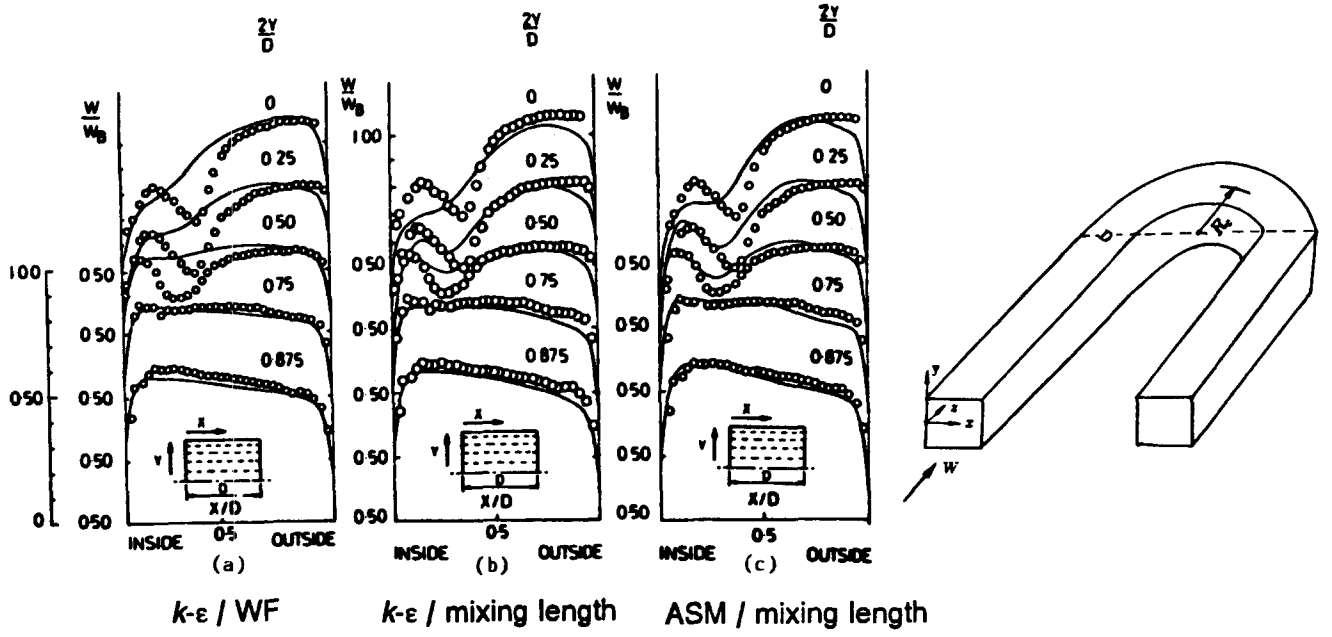

Figure 8 Axial velocity comparisons for flow through a U-duct of curvature ratio of, R_c/D, of 3.375 at $\theta = 90°$

spite a coarse grid and, apparently, the omission of viscosity–gradient terms from the transport equations, encouraging agreement was achieved with global heat transfer and friction-factor data. Iacovides and Launder (1987a) re-examined this rotating pipe geometry, albeit simply fully developed flow, adopting both the k-ε/mixing-length model and also the ASM scheme (again interfaced with the mixing length model across the sublayer). Figures 1 and 2 (from Iacovides and Launder 1987a) show that there are rather small differences in the predicted wall shear stresses between the eddy-viscosity model (EVM) and ASM treatments, both giving satisfactory agreement with Ito and Nanbu's (1971) experimental correlation. An analogous study of a square-sectioned pipe (Iacovides and Launder 1987b), brought out a considerable sensitivity of the results to mesh distribution, linked to the fact that, for Ro = 0.2, an additional small counter-rotating eddy is formed on the pressure surface rotating in the opposite sense to the primary eddy. If a too strongly nonuniform mesh were used, this secondary eddy would be suppressed. Again, rather little difference between overall thermal and dynamic fields resulted from using an ASM in the core rather than an EVM, a result that helps underline the importance of the sublayer where, in both cases, the mixing length scheme was adopted. Further explorations of the effects of duct aspect ratio for fully developed flow have subsequently been explored by the authors (Iacovides and Launder 1991) and Bo (1992). From the latter study, the great sensitivity of the predicted flow behavior to initial conditions emerged. This is illustrated in Figure 3 where, for a duct with 2:1 aspect ratio, over a range from $0.04 < \mathrm{Ro} < 0.11$, one could obtain either a one-vortex or a two-vortex pattern, depending on initial conditions.

In the case of flow through actual blade-cooling passages, the large near-wall density gradients, combined with the intense centrifugal acceleration, bring an additional factor (the rotational Rayleigh number) into account. Studies by Iacovides and Launder (1987a) provided the first computations including buoyant effects, albeit for the case of a circular pipe. Now, the radial pressure gradient induced by rotation is $\bar{\rho}\Omega^2/R$ ($\bar{\rho}$ being the average density over the cross section), and this is greater than the low-density near-wall fluid requires to describe a circular path (i.e., $\rho\Omega^2/R$). Thus, if there were no net flow along the tube, the near-wall fluid would move inward (to smaller radii), and that near the axis would move outward. If this effect is superimposed on the forced convection motion, it is evident that, for radially outward flow, buoyancy will enhance the difference between the near-wall and central velocities; while, for inward flow, the reverse will occur. In fact, there are secondary effects, because the modification to the axial velocity in turn alters the Coriolis force. Nevertheless, the computational results (Figure 4) indicate modifications to the velocity field broadly in line with the above first-order inferences.

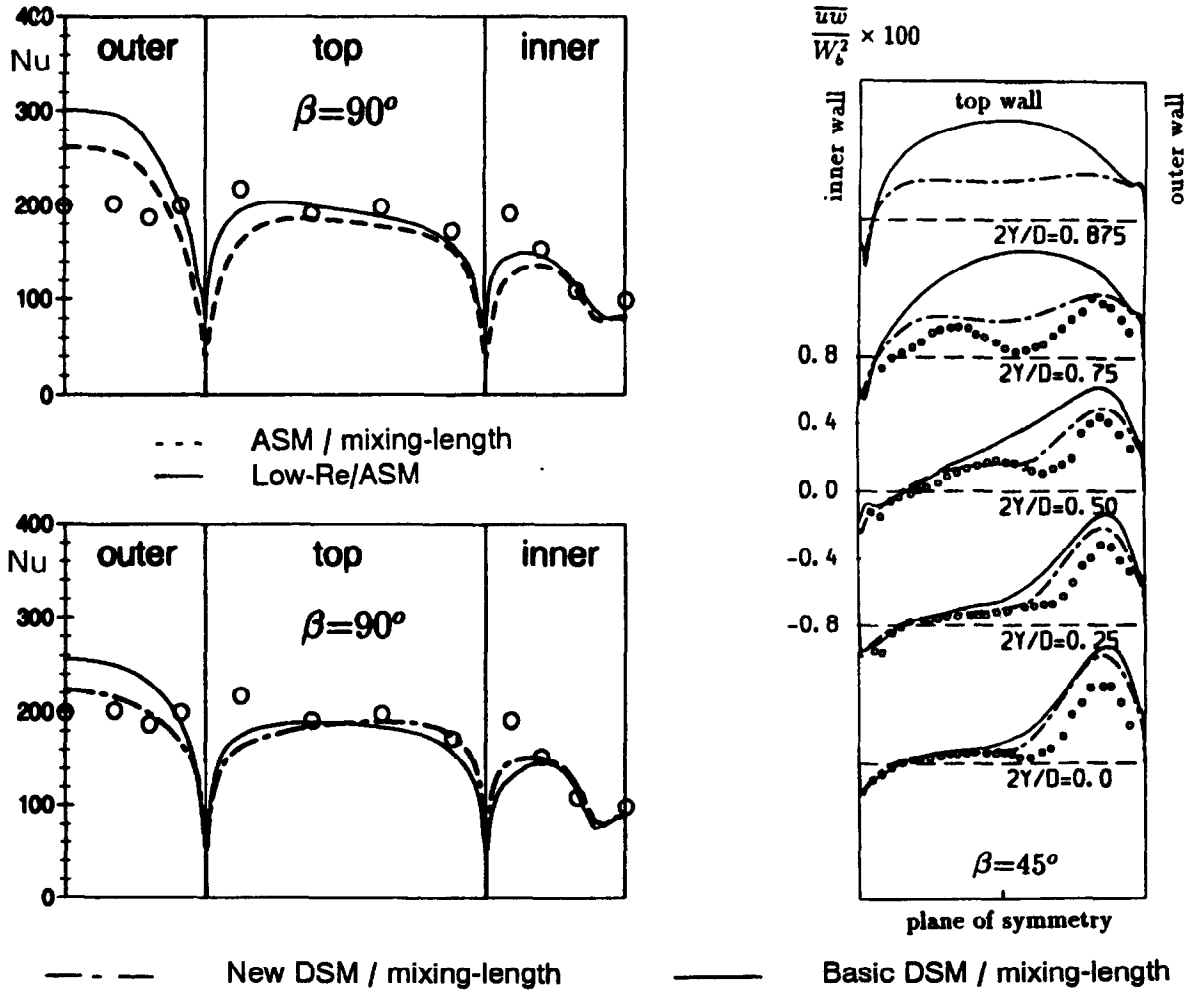

Figure 9 Nusselt number comparisons for flow through a U-duct of curvature ratio of 3.375 at $\theta = 90°$ and turbulent shear stress comparisons at $\theta = 45°$

The first experimental data (for a square-sectioned duct) decisively distinguishing Coriolis and buoyant effects appeared a little later (Wagner et al. 1989). Although the data were limited to side-averaged values of Nusselt number, they have been very helpful in allowing discrimination between alternative turbulence models. Prakash and Zerkle (1992) computed a number of these cases using the high-Re k-ε model with the wall function approximation. This model was able to reproduce the main effects of rotation on wall heat transfer, but the authors acknowledged that further refinements to the turbulence model were required. The use of an EVM scheme comprising a one-equation model across the near-wall sublayer and a k-ε scheme over the rest of the duct (Bo et al. 1991) proved to be moderately successful in capturing the thermal field development (Figure 5). What was particularly striking was the large difference between the computed variation of Nusselt number, depending on whether density variations were or were not included. However, it appeared that on the suction side, the predicted mean heat transfer coefficient was 30–60% above measured values. Accordingly, model refinement was undertaken (Bo et al. 1995a). First experiences were not encouraging, because on the suction side of the duct, predicted levels with a low-Reynolds number k-ε scheme (not shown) were higher than for the nonrotating duct. Thereafter, a low-Reynolds-number ASM, developed to improve bend-flow predictions, was employed, and this led to marked improvement (Figure 6). A particularly striking result was that, on the suction side, rapid variations in Nusselt number occurred between five and ten diameters downstream, a feature associated, in the computations, with the formation and subsequent disappearance of an additional secondary eddy attached to the suction surface. Although the spacing of the experimental data is too large to be certain that the predicted phenomena are, in fact, observed, we can say that the predictions are at least reasonably consistent with the experimental data.

Flow and heat transfer in U-bends

Although, in practice, the radii of U-bends encountered in cooling is usually less than the passage diameter, we begin by considering briefly somewhat less severe bends where separation does not occur. During the 1980s, our group's efforts were focused on circular- and square-sectioned U-bends of curvature ratio, R_c/D of 3.38 because of the availability of flow and heat transfer data for these cases. As in a rotating duct, the square cross section — both from numerical and modeling standpoints — is substantially the more difficult case and it is mainly this with which comparisons are drawn.

The cross-duct pressure gradient arising from streamline curvature induces, just as in orthogonal rotation, a secondary motion that carries high momentum core fluid toward the outside of the

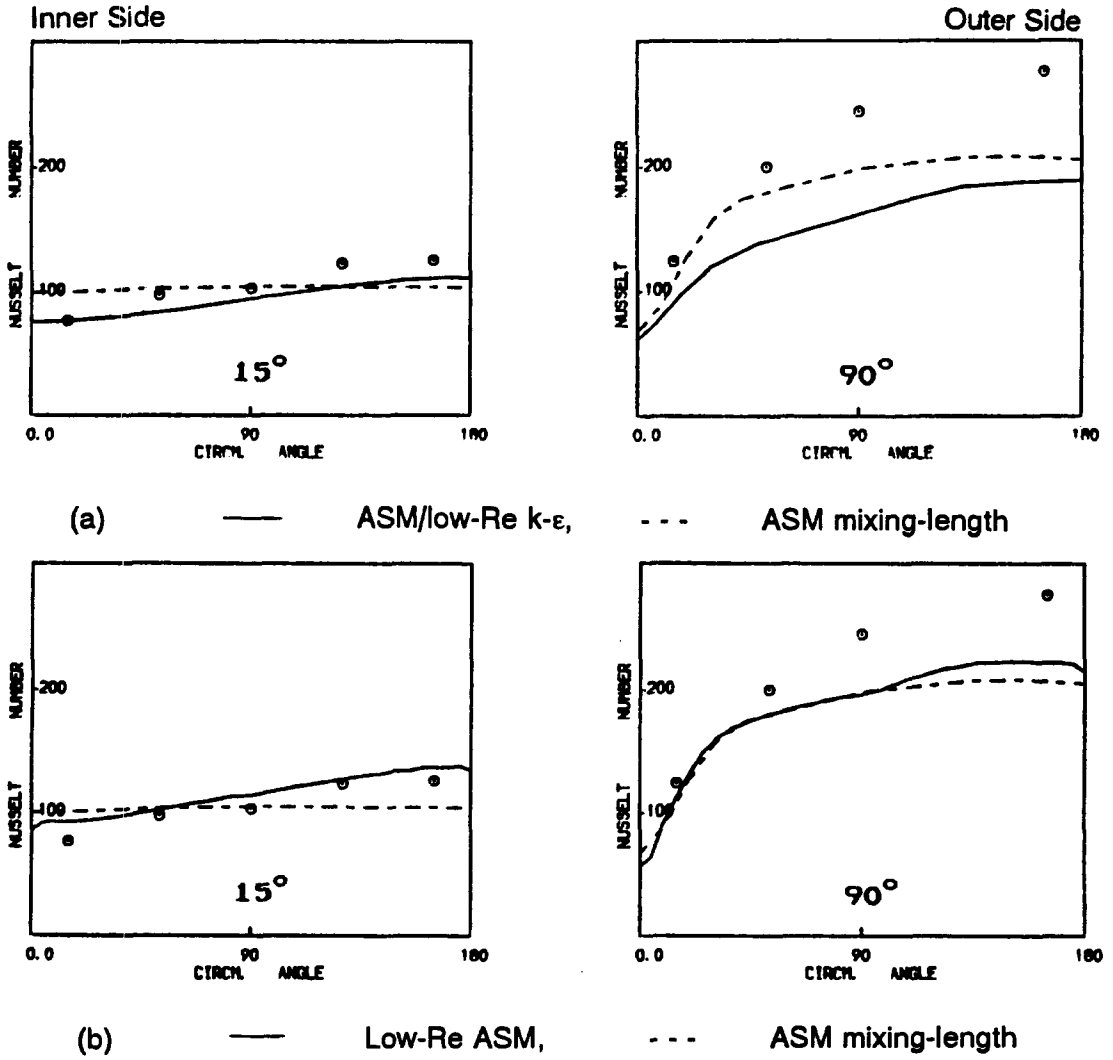

Figure 10 Circumferential distribution of the local Nusselt number for flow through a circular U-bend of curvature ratio of 3.375

bend with an intense return flow very close to the wall where the slow moving fluid is driven radially inwards. Although it is usual to sketch this flow as a simple single vortex (as arises in laminar flow at low Dean numbers), in turbulent flow, it is usually far more complex. Now, the *predicted* secondary flow pattern depends crucially on the modeling strategy adopted, as shown in Figure 7, drawn from the work of Choi et al. (1989). A k-ε EVM with wall functions, Figure 7 leads to a double-cell arrangement; whereas, with the wall functions replaced by a fine-grid, mixing-length treatment, an additional discrete vortex appears. Finally, the refinement of the core turbulence model from an EVM to an ASM produces a further vortex and, moreover, noticeable changes in the shape of the vortices. These changes in the secondary motion produce successive clear-cut improvements in the agreement with the measured streamwise velocity field (Figure 8). Very recently, Li (1995) has repeated computations of this flow using a *differential* rather than an algebraic stress model in the core and employing one of the new closures that require no wall reflection terms. She found a number of clear-cut improvements over the best results of Choi et al (1989) both in the dynamic field and, moreover, in the resultant heat transfer predictions (Figure 9). We note, finally, in relation to this test case, that Breuer and Rodi (1994) have reported a large-eddy simulation (LES) of the flow. Although agreement with experiment was less close than achieved by either ASM or differential second-moment (DSM) computations noted above, it provides a pointer for possible directions of further development.

Another comprehensive set of U-bend heat transfer comparisons has been made for the case of a circular cross section. It is seen from Figure 10a that refining the near-wall model from a mixing-length EVM to a two-equation k-ε (Iacovides and Launder 1992) improves the bend entry behavior, but gives worse agreement than even the mixing-length hypothesis at 90°. The circumferential nonuniformity in Nu at the bend entry is due to the partial laminarization of the boundary layer on the inside of the bend arising from the strong acceleration in this region. The introduction of the low-Re ASM (Figure 10b) leads to closer accord with the data in the entry region and also at the 90° location, although, at this position, the augmentation of Nu on the outside of the bend is still underestimated. As already shown in Figure 9, this model overestimates heat transfer levels at the corresponding location of the U-bend of square cross-section. This difference in the model's performance for these two geometries can be attributed partially to the fact that in the rectangular duct (see Figure 7) there is a far stronger secondary flow impingement on the pressure surface. The "standard" wall reflection terms contained in the ASM model employed are known to predict excessive Nusselt numbers in regions of flow impingement.

We turn now to flows around the much tighter U-bends found in gas-turbine practice where, because of the more severe adverse pressure gradient on the inside of the bend in the vicinity of exit, a downstream recirculating flow zone is created. One of the first computational studies in such a configuration with $R_c/D = 1.59$ was by Besserman and Tanrikut (1991). They employed the k-ε model in the core coupled with either the wall-function approximation or, as recommended earlier by Choi et al. (1989), with the flow equations integrated across the sublayer using the Van Driest (1956) mixing length model. In conformity with the earlier unseparated flow studies, the latter approach was found to give emphatically better agreement with measured Nusselt number distributions.

Computations of flow and heat transfer in tighter U-bends have recently been carried out by Xia and Taylor (1993) and Bo et al. (1995b). The former employed a curvature-modified mixing-length hypothesis for a bend with $R_c/D = 0.5$, achieving generally satisfactory predictions of side-averaged heat transfer. The more extensive explorations of Bo et al. (1995a, b) focused first on the question of securing grid independence, exploring in the process different strategies for discretizing convective transport. It emerged that even with (by today's standards) a fine mesh (35×67 mapping the half cross section and with 130 streamwise planes) it was essential to employ a higher-order treatment of convection, such as LODA (Zhou and Leschziner 1988) *even on the turbulence variables* k and ε (Figure 11). This finding is at variance with conventional wisdom, which regards simple upwind differencing of the turbulence quantities as adequate, because convection is supposed to play a relatively minor role (compared with sources and sinks) in those equations. The difference in the present flow causing the unexpected result was that the downstream behavior is extremely sensitive to small changes in the position of the separation point, which, in turn, is highly dependent on the levels of k and ε approaching separation. Now, in the vicinity of the separation point, turbulence production of energy near the wall is a relatively minor contributor, and, of necessity, convection is of rather greater importance. That seems to be why the higher-order treatment of convection of k and ε is so important.

We note that with LODA on all variables, besides achieving sensible grid independence, satisfactory agreement is also

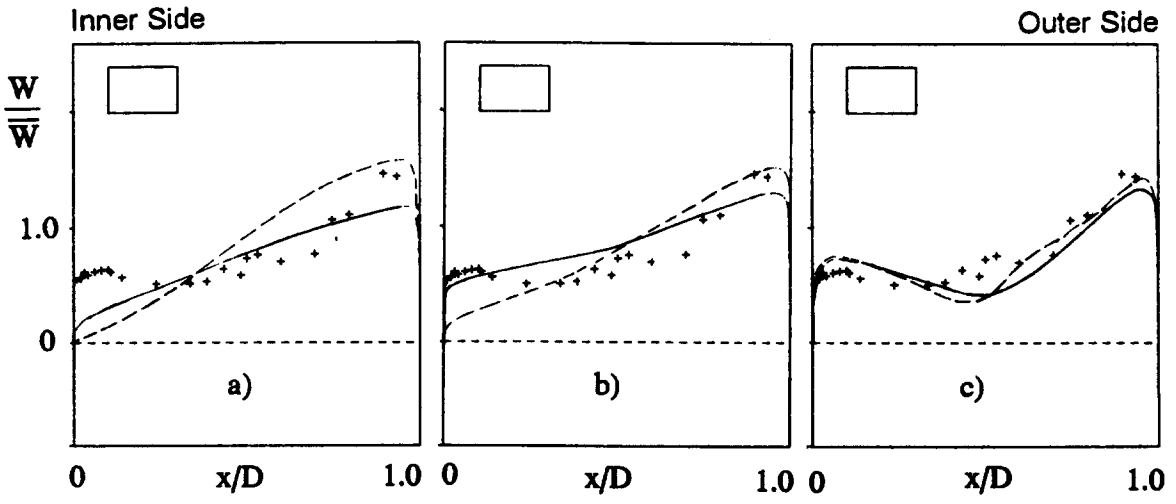

Figure 11 Effects of convective discretization on flow predictions three diameters downstream of a U-bend of curvature ratio of 0.65; ----- $35 \times 67 \times 103$; ——— $35 \times 67 \times 130$; (a) HYBRID; (b) LODA on all but ε; (c) LODA

achieved with the velocity measurements of Hicklin (1988). Agreement is also satisfactory with the measured heat transfer coefficients on the top wall of the U-bend (Figure 12). However, accord is much less satisfactory along the inner and outer walls, especially in and immediately downstream of regions where the near-wall flow is rapidly accelerated. It is known from simpler 2-D boundary layers, that in such regions, a thickening of the viscous sublayer occurs, and this suggests that solving a transport equation for ε all the way to the wall is essential to mimic the flow behavior correctly.

Recently, a more detailed laser Doppler anenometry (LDA) mapping of the flow field in a U-bend with $R_c/D = 0.65$ (Cheah et al. 1994) has stimulated further exploration of more advanced modeling treatments. In Iacovides et al. (1995) the usual ASM closure was first employed to replace the EVM in the core, and subsequently, the ASM was also extended to the near-wall sublayer. As Figure 13 shows, these refinements produce clear improvements in the predicted behavior, although it may be noted that the best scheme only manages to remove about half the difference in velocity between the k-ε/one-eq computations and the measurements.

Rotating U-bends

In blade cooling, the axis of curvature of the coolant passages is roughly perpendicular to the rotation axis of the blades. Consideration of this case was recently reported by Sathyamurthy et al. (1994). Although the simple turbulence model (k-ε EVM + wall functions) is unlikely to have achieved great accuracy, it is, nevertheless, of interest to note in Figure 14 the complex predicted flow pattern, entirely lacking any symmetry surface, that develops downstream of the bend.

The only known case where, for a rotating U-bend, flow measurement and computation can be compared is for a situation where the rotation axis of the duct and bend axis are parallel (Cheah et al. 1994). Then, there is geometric symmetry about the duct's midplane, and, if we believe the flow will respect that symmetry, computations can be confined to one half of the duct. In this configuration, the flow structure differs according to whether the outer (pressure) side of the bend does or does not coincide with the pressure side due to rotation; in other words, whether the secondary flows created by curvature and rotation reinforce or oppose one another (situations labeled positive or negative rotation, respectively). Computations of this flow have been provided by Iacovides et al. (1995), employing the low-Re ASM that had performed best in the stationary bend considered above (Figure 15). For the case of positive rotation, there is encouraging agreement between the measurement and prediction of both mean flow and the turbulent stress field. For negative rotation, however, while the main features are captured, there are more substantial differences between the measured and predicted development downstream of the bend.

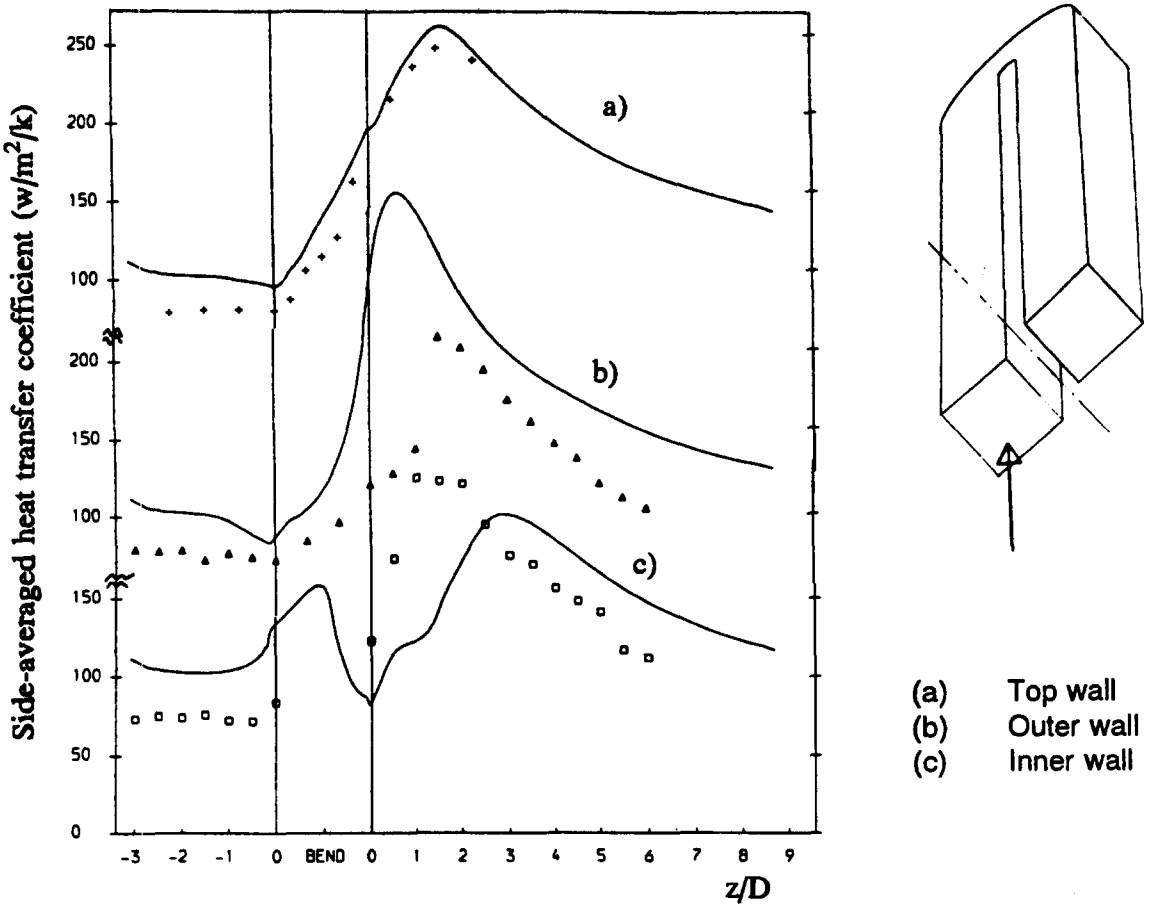

Figure 12 Development of side-averaged heat transfer coefficient around a U-duct of curvature ratio of 0.65

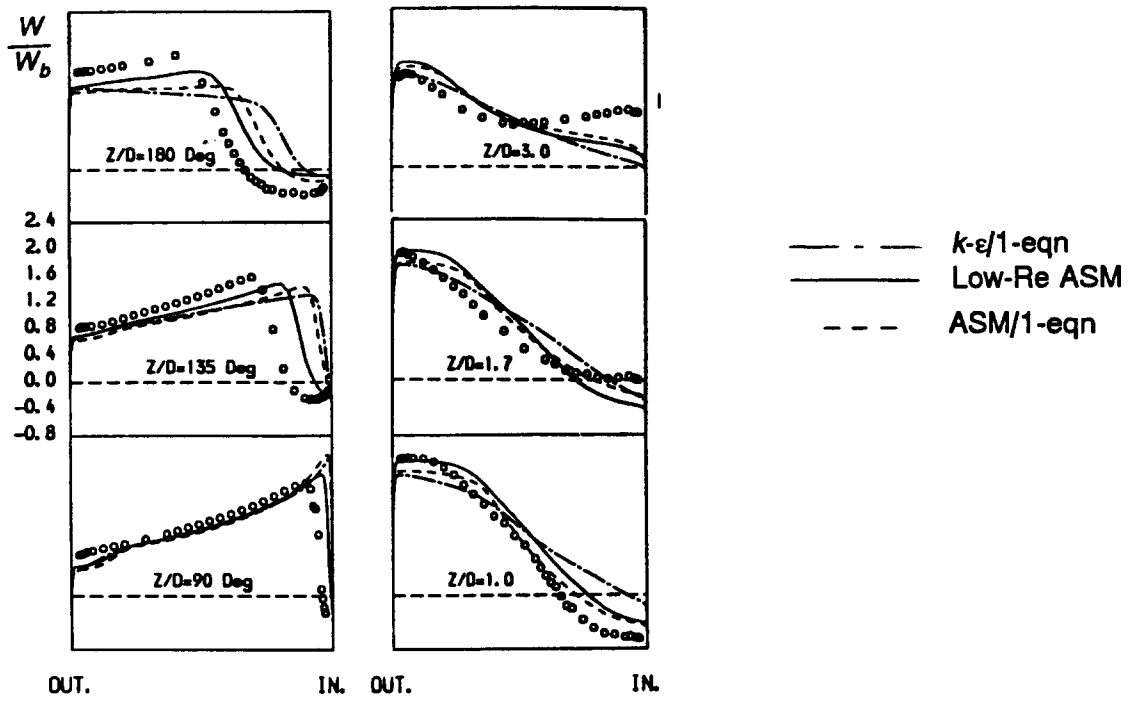

Figure 13 Comparisons of axial velocity profiles along the symmetry plane of a U-duct of curvature ratio of 0.65

Computations of flow and heat transfer through ribbed passages

There have been many computational studies of the flow over square or rectangular roughness elements ranging from the initial one-equation study of Shah (1971) to the ASM computations of Liou et al. (1993). The aim of this work has been mainly to predict the effect of the ribs on the convective heat transfer coefficient.

Of course, the performance of the ribs will be greatly affected by the strong secondary flows present in the blade-cooling passages, especially because the secondary flow is strongest close to the wall. Thus, it seems quite uncertain what inferences can be drawn from simple 2-D studies that could be applied to rotating channels. The only study of flow through a rotating ribbed channel seems to be that of Taylor et al. (1991). To be consistent with the conditions of their experiments, the thermal energy equation was solved within the pipe wall as well as within the flow. Using a high-Re k-ε EVM they felt that, for values of Ro up to 0.12, the predicted behavior was reasonable; however, they acknowledged that further consideration of modeling issues was necessary. Certainly, the study of the effect of ribs on the flow in rotating U-bends is the last piece of the jigsaw to put into place. We can expect several computational studies, employing more widely applicable modeling strategies, to be undertaken in the next year or two.

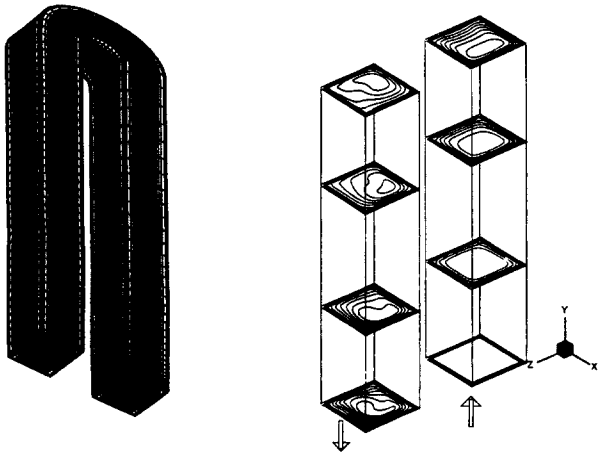

Figure 14 Temperature contours within a rotating U-duct, where the axis of rotation is normal to the axis of curvature

Computation of flow and heat transfer through rotating disc cavities

The overall cooling system of gas-turbine plants also involves flow and heat transfer through cylindrical cavities formed between adjacent discs. With rare exceptions, most experimental and theoretical studies have considered idealized cases of axisymmetric cavity flows. Even within this constraint, however, a variety of cavity flows has been investigated because of the different flow configurations that can exist within a gas-turbine system. Among the types that are relevant to gas-turbine cooling applications are co-rotating discs with either radial outflow, as shown in Figure 16a, or radial inflow, a co-rotating system with axial throughflow, as shown in Figure 16b, a rotor–stator system without throughflow, a rotor–stator system with radial outflow, as shown in Figure 16c, a rotor–stator system with radial inflow and, as shown in Figure 16d, a counter-rotating system with and without throughflow. The common characteristic of all rotating cavity flows is that, due to the difference in the rotational speed of the near-wall and the core fluid, Ekman-type boundary layers are formed along the disc surfaces, pumping the fluid either inward or outward, depending on whether the disc rotates faster or slower than the core fluid. This is illustrated in Figure 17 for a rotor–stator system. Beyond this common characteristic, a variety of other flow features can be present in different types of cavity flows. In enclosed systems with no throughflow and also in some systems with radial outflow, the flow near the axis of the cavity is usually laminar. As a result, the outward-moving boundary

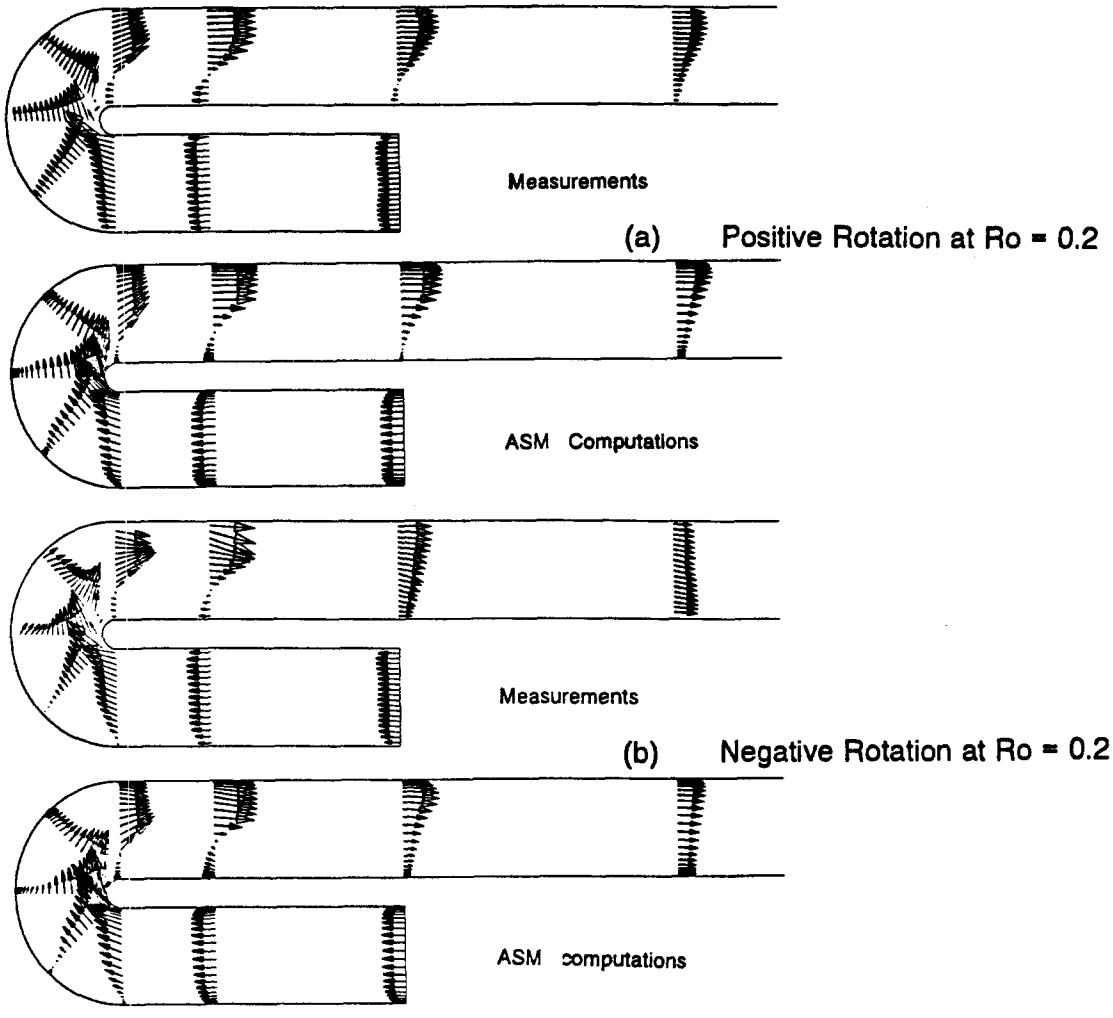

Figure 15 Mean flow comparisons along the symmetry plane of a rotating U-duct of curvature ratio of 0.65

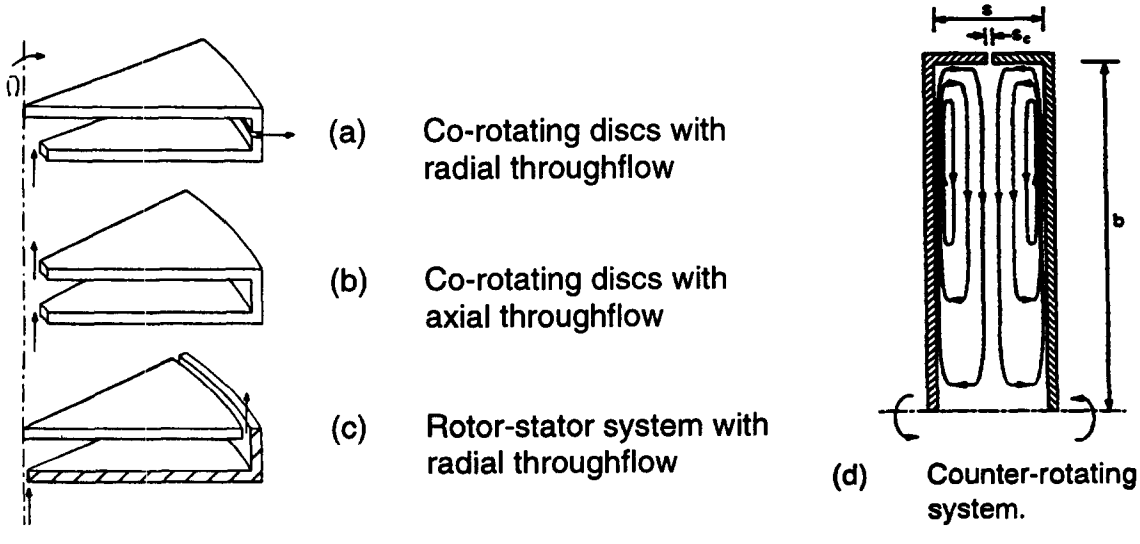

Figure 16 Types of rotating cavity flows

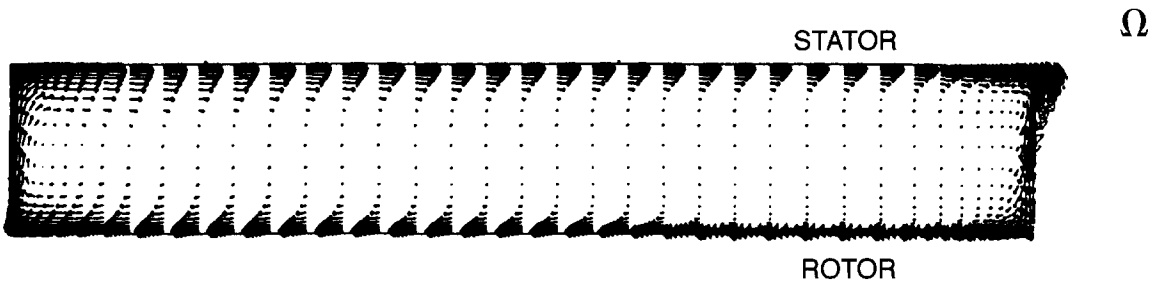

Figure 17 Radial flow in a rotor–stator system without throughflow

layer along the rotating disc, starts out laminar and then, as the radius increases, becomes turbulent. Systems with no throughflow and also systems with axial inlet flow include the phenomenon of flow impingement, while cavities with axial throughflow involve flow entrainment. In heated cavities, rotational buoyancy effects may also be significant. As shown in the recent experimental work of Debuchy (1993), radial inflow leads to the convection of high turbulence levels into the inner region of the cavity. This variety of flow features may explain why numerous turbulence models have been applied to the computation of cavity flows, with different researchers arriving at different conclusions.

Initial attempts by Chew (1984) to compute cavity flows, using the high-Re k-ε model with the wall function approximation, failed to reproduce major flow characteristics. Subsequently, Chew (1985) and Chew and Vaughan (1988) showed that use of low-Re mixing-length models, in which the flow equations are integrated over the wall sublayer regions, led to more reasonable flow predictions both for co-rotating discs with radial outflow and for rotor–stator systems. The critical influence of the near-wall regions and the consequent need to account correctly for the near-wall processes was further emphasized by Iacovides and Theofanopoulos (1991). A zonal modeling approach was employed in which either a high-Re k-ε, or an ASM model was employed in the cavity core with different versions of the mixing-length model in the near-wall regions. This approach returned satisfactory predictions for co-rotating disc flows and also for rotor–stator flows. However, as seen in Figure 18, due to the limitations of the near-wall model, different versions of the mixing-length hypothesis gave better agreement for different types of disc flows. The zonal modeling approach was further tested by Iacovides and Chew (1993) in the prediction of heat transfer through cavities involving either radial outflow or axial throughflow. The zonal approach gave better heat transfer predictions than when the mixing-length model was employed over the entire cavity. The low-Re one-equation model emerged, however, as the most reliable of the near-wall models tested (Figure 19), although even this approach had its limitations, especially for cases involving axial throughflow. A more recent investigation by Virr et al (1993), has claimed that, in some cases, provided the rotational Reynolds number is high enough and particular

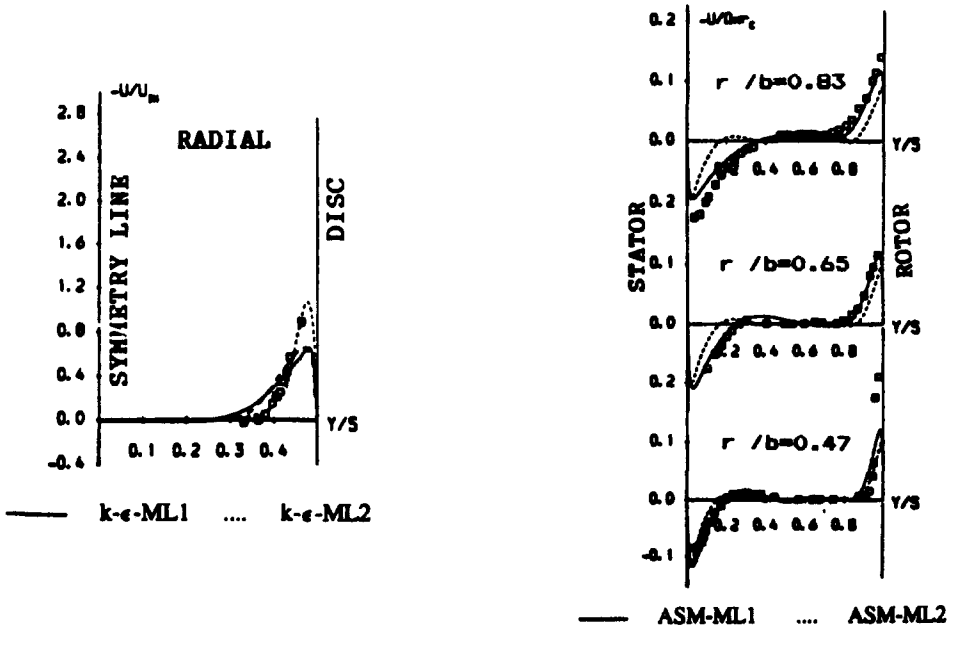

(a) Co-rotating discs (b) Rotor-stator system

Figure 18 Comparisons of radial velocity profiles using zonal modelling approach, for rotating cavities; ML1:Van Driest mixing length; ML2:Koosinlin mixing length

care is taken in the distribution of the near-wall grid nodes, the wall function approach can also be made to work. The zonal k-ε/one-eq model was found to have greater generality, however.

Extensive efforts to employ a low-Re k-ε model for the computation of rotating cavity flows have been made by Morse and his co-workers. The Launder and Sharma (1974) low-Re k-ε model, when tested in co-rotating disc flows (Morse 1988), was found to predict too large a laminarized region over the inner region of the cavity. To overcome this problem, Morse (1988) introduced an extra negative source term in the dissipation transport equation, a wall-distance-dependent damping function for the turbulent viscosity and, in the production term of the turbulent kinetic energy, he included a small fraction of the turbulent viscosity as calculated by the mixing length model. These modifications resulted in satisfactory predictions of flow and heat transfer through co-rotating disc flows, (Morse 1991a; Morse and Ong 1992) and also of flow through rotor–stator systems (Morse 1991b).

In a subsequent study of buoyancy-affected flow in asymmetrically heated cavities, Long et al. (1993) found it necessary to calculate the main component of the turbulent shear stress from an ASM equation. The Morse model was also successfully employed in the computation of flow and heat transfer through rotor–stator systems by Chen et al. (1994). The same group, however (Kilic et al. 1994), found the original Launder and Sharma (1974) model to be more suitable for the computation of flow through counter-rotating systems, although for some counter-rotating disc cases with radial outflow (Gan et al. 1994), this model again produced unrealistically large boundary-layer regions.

The recent emergence of detailed flow measurements for rotor stator systems (Itoh et al. 1990; Cheah et al. 1994), provided our group with the opportunity to test a number of low-Re models for this type of flow (Iacovides and Toumpanakis 1993). A zonal k-ε/one-eq model and the Wilcox k-ω model were shown to be unable to predict the laminar flow regions at the center of the cavity. As shown earlier by Morse, the Launder–Sharma (1974) low-Re k-ε model and also a low-Re differential stress model (DSM) predicted laminar flow regions larger than indicated in the corresponding measurements. In the vicinity of the outer shroud, where flow impingement takes place, it was shown that the use of the Yap length scale correction term was necessary for the two low-Re models (k-ε and DSM). This need was greater in the case of the low-Re k-ε model. The problem of delayed transition was addressed by introducing a modification to the ε equation, which, when the fluid was in solid-body rotation, reduced the dissipation rate of turbulence. This was an empirical, albeit coordinate invariant, way of making the turbulence equation sensitive to the fact that solid-body rotation reduces the break-up of large-scale turbulent eddies; this was especially effective at low rotation Reynolds numbers (Figure 20). In a subsequent study, Te Braak (1994) limited the effects of solid-body rotation to regions of low-Reynolds number turbulence. As shown by Te Braak and Nikas (1995), with this modification, the Launder and Sharma (1974) low-Re k-ε model and the low-Re DSM of Iacovides and Toumpanakis (1993) were able to return reasonable flow predictions over a range of cavity flows including rotor–stator systems with radial outflow or inflow, co-rotating disc systems with radial outflow, and counter-rotating disc systems with radial outflow. In some of these cases, use of a low-Re DSM closure led to additional improvements in the predictions.

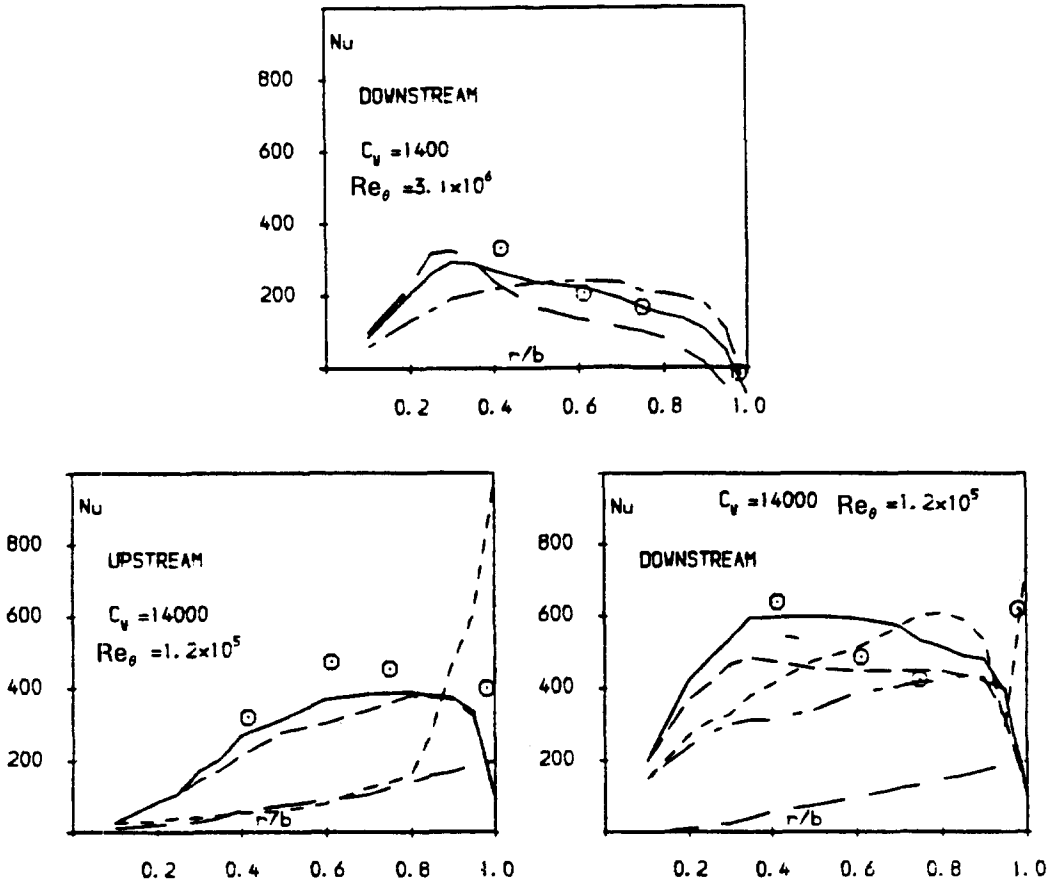

Figure 19 Nusselt number comparisons for a rotating cavity with radial outflow; ——— k-ε/1-eq; ----- k-ε/ML1; — — — k-ε/ML2; ····· mixing length; — — integral method

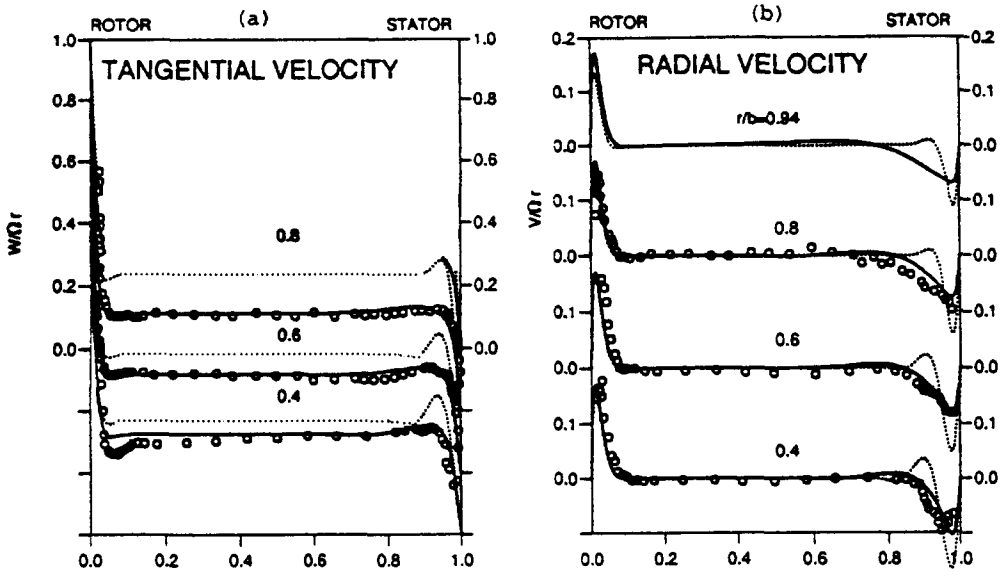

Figure 20 Effect of rotation modification to the ε equation on the prediction of a rotor–stator flow at $S/b = 0.127$ and $Re_\theta = 0.3 \times 10^6$; ----- Launder and Sharma 1974 Low-Re k-ε; ——— modified Launder and Sharma k-ε

Attempts to apply other low-Re k-ε models have also been reported by Louis and Salhi (1988) and Ton and Lin (1994), but only a limited number of flow cases have been considered.

Finally, further applications of second-moment closures to the computation of rotating disc flows have been reported by researchers from the Marseille Fluid Mechanics Institute. Elena and Schiestel (1993) and Schiestel et al. (1993) initially employed a zonal modeling approach in which an ASM model was used in the core region of the cavity with the Launder and Sharma (1974) k-ε model within the near-wall regions. This approach gave satisfactory flow predictions for rotor–stator flows and also for co-rotating disc flows with radial outflow. Subsequently, Elena (1994) employed variants and of the new low-Re differential stress models not requiring wall-reflection agencies but to which he had added a set of extra rotation-related terms. The first of these models was shown to be successful both for co-rotating disc flows with radial outflow and for rotor-stator flows with and without radial outflow, while the second was tested in the computation of two rotor–stator flows without throughflow. As shown in Figure 21, these second-moment closures achieved very good agreement with available measurements. Their application to a wider range of cavity flows is, however, necessary to assess fully their effectiveness in the prediction of practically relevant cases.

Conclusions

This rapid skim through some of the flows related to the cooling of hot-section components has brought out the following:

(1) There are few flows where adequate predicted behavior can be achieved using wall functions to bridge the viscosity-affected sublayer. Even if only a mixing length scheme is used there, the computed behavior using a low-Reynolds-number turbulence model is far more reliable.

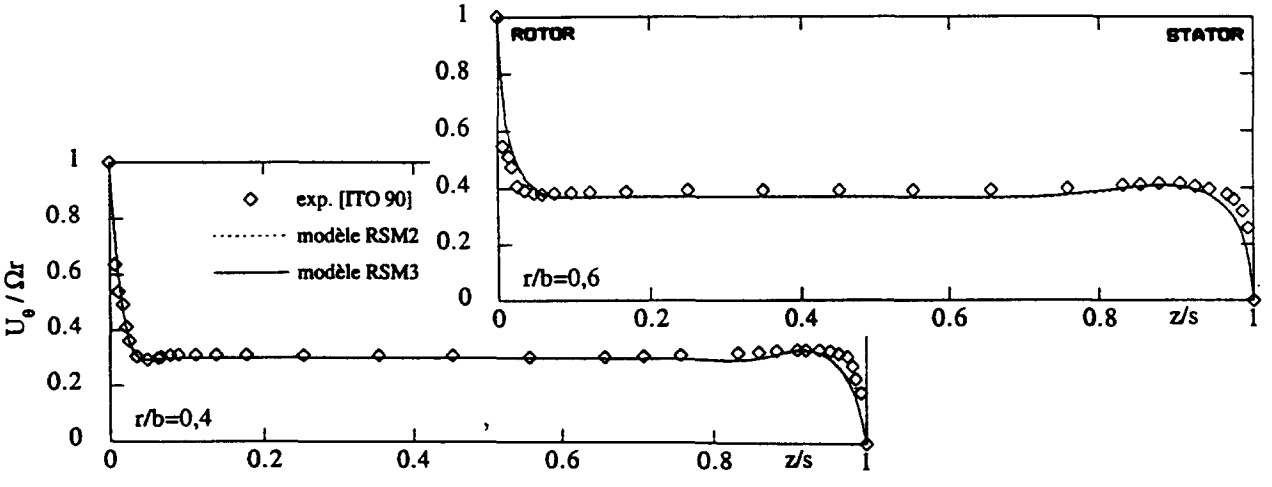

Figure 21 Tangential velocity comparisons for a rotor–stator flow at $S/b = 0.08$ and $Re_\theta = 10^6$ for the Elena low-Re stress models

(2) The use of a two-equation linear eddy-viscosity model in the turbulent core coupled with a simpler one-equation model across the sublayer provides a useful route for tackling most of the flows considered. Although this may not achieve the highest-quality prediction, it is a straightforward level of modeling to use and has a good track record for capturing the broad trends.
(3) Second-moment closure emerged as the route giving the best agreement with experiment, despite the problems and ambiguities over the application of the wall reflection terms.

For the future, we see practical predictions following one of two new routes: either to adopt one of the new *nonlinear* eddy-viscosity models that captures the sensitivity of turbulence to streamline curvature fairly well, or to employ a second-moment closure that does not require wall-reflection terms. Both approaches have been subjected to a fair amount of testing in 2-D shear, and the latter has begun to be tried in cooling studies. It is now time that each was systematically applied to the range of flows considered in this paper to validate and, where necessary, to refine them prior to their use in industrial design.

Acknowledgments

The authors express their appreciation to all their co-workers at UMIST whose names appear in the reference list and to Rolls-Royce PLC and RAE Pyestock who have provided the principal funding for the research. Mr. M. J. Newman has prepared the camera-ready manuscript with appreciated care. Authors' names appear alphabetically.

References

Besserman, D. L. and Tanrikut, S. 1991. Comparison of heat transfer measurements with computations for turbulent flow around a 180° bend, *Proc. Int. Gas-Turb. and Aero Congress* (ASME Paper 91-GT-2), Orlando, FL

Bo, T., Iacovides, H. and Launder, B. E. 1991. The prediction of convective heat transfer in rotating square ducts. *Proc. 8th Int. Symp. on Turb. Shear Flows*, Munich, Germany

Bo, T., 1992. The computation of flow and heat transfer in rotating ducts and U-bends. Ph. D. Thesis, Faculty of Technology, University of Manchester, Manchester, UK

Bo, T., Iacovides, H. and Launder, B. E. 1995a. Developing buoyancy-modified turbulent flow in ducts rotating in orthogonal mode. *Turbomachinery*, **117**, 474–484.

Bo, T., Iacovides, H. and Launder, B. E. 1995b. Convective discretization schemes for the turbulence transport equations in flow predictions through sharp U-bends. *Int. J. Num. Meth. Heat Fluid Flow*, **5**, 33–48

Bradshaw, P. 1973. Effects of streamline curvature on turbulent flow. AGARDograph 169

Breuer, M. and Rodi, W. 1994. Large-eddy simulation of turbulent flow through a straight square duct and a 180° bend. *1st ERCOFTAC Workshop on Direct and Large-Eddy Simulations*, **3**, University of Surrey, Surrey, UK

Cheah, S. C., Iacovides, H., Jackson, D. C., Ji, H. and Launder, B. E. 1994a. LDA Investigation of the flow development through rotating U-ducts. *Proc. Int. Gas-Turb. and Aero Congress* (ASME Paper 94-GT-226), The Hague, The Netherlands

Cheah, S. C., Iacovides, H., Jackson, D. C., Ji, H. and Launder, B. E. 1994e. Experimental investigation of enclosed rotor–stator disc flows. *Exp. Thermal and Fluid Sci.* **9**, 445–455

Chen, J. X., Gan, X. and Owen, J. M. 1994. Heat transfer in an air-cooled rotor–stator system. *Proc. Int. Gas-Turb. and Aero Congress* (ASME Paper 94-GT-55), The Hague, The Netherlands

Chew, J. W. 1984. Prediction of flow in rotating disc systems using the k-ε turbulence model. *Proc. Int. Gas-Turb. and Aero Congress* (ASME Paper 84-GT-229). The Hague, The Netherlands

Chew, J. W. 1985. Prediction of flow in a rotating cavity with radial outflow using a mixing length model of turbulence. *Proc. 4th Int. Conference on Numerical Methods in Laminar and Turbulent Flows*, Swansea, Wales

Chew, J. W. and Vaughan, C. M. 1988. Numerical predictions of the flow induced by an enclosed rotating disc. *Proc. Int. Gas-Turb. and Aero Congress* (ASME Paper 88-GT-127), Amsterdam, The Netherlands

Choi, Y- D., Iacovides, H. and Launder, B. E. 1989. Numerical computation of turbulent flow in a square-sectioned 180° bend. *J. Fluids Eng.*, **111**, 59–68

Craft, T. J., Launder, B. E. and Suga, K. 1993. Extending the applicability of eddy-viscosity models through the use of deformation invariants and non-linear elements, *Proc. 5th IAHR Conference on Refined Flow Modelling and Turbulence Measurement*, Paris, France

Debuchy, R. 1993. Ecoulement turbulent avec inspiration radiale entre un disque fixe et un disque en rotation. (Ph. D.) thesis, Université des Sciences et Technologie de Lille, Lille, France

Elena, L. and Schiestel, R. 1993. Numerical prediction of turbulent flow in rotor–stator systems. In, *Engineering Turbulence Modelling and Experiments 2*, W. Rodi and F. Martelli (eds.), Elsevier, New York

Elena, L. 1994. Modelisation de la turbulence inhomogène en présence de rotation. (Ph. D.) thesis, Université d'Aix Marseille II, Marseille, France

Fu, S., Launder, B. E. and Leschziner, M. A. 1987, Modeling strongly swirling recirculating jet flow with Reynolds-stress transport closures. *Proc. 6th Symposium on Turbulent Shear Flows* (Paper 17.6), Toulouse, France

Gan, X., Kilic, M. and Owen, J. M. 1994. Superposed flow between two discs contrarotating at differential speeds. *Int. J. Heat Fluid Flow*, **15**, 438–446

Howard, J. H. G., Patankar, S. V. and Bordynuik, R. M. 1980. Flow prediction in rotating ducts using Coriolis-modified turbulence models. *J. Fluids Eng.*, **102**, 456–461

Hicklin, D. J. 1988. Experimental velocity and turbulence measurements in a perspex 180° bend model using a polytec laser anemometer. Rolls-Royce internal report, GN29335

Iacovides, H. and Chew, J. W. 1993. The computation of convective heat transfer in rotating cavities. *Int. J. Heat Fluid Flow*, **14**, 146–154

Iacovides, H. and Launder, B. E. 1987a. Turbulent momentum and heat transport in square-sectioned ducts rotating in orthogonal mode. *Num. Heat. Transfer*, **12**, 475–491

Iacovides, H. and Launder, B. E. 1987b. The numerical simulation of flow and heat transfer in tubes in orthogonal-mode rotation. *Proc. 6th Int. Symposium on Turbulent Shear Flows*, Toulouse, France

Iacovides, H. and Launder, B. E. 1991. Parametric numerical study of fully developed flow and heat transfer in rotating rectangular ducts. *J. Turbomachinery*, **113**, 331–338

Iacovides, H. and Launder, B. E. 1992. The computation of convective heat transfer in a 180° pipe bend, ICHMT *Int. Symposium on Heat Transfer in Turbomachinery*, Athens, Greece

Iacovides, H., Launder, B. E. and Li, H- Y. 1995. The computation of flow development through stationary and rotating U-bends of strong curvature. *Int. J. Heat Fluid Flow*, to appear

Iacovides, H. and Theofanopoulos, I. P. 1991. Turbulence modeling of axisymmetric flow inside rotating cavities. *Int. J. Heat Fluid Flow*, **12**, 2–11

Iacovides, H. and Toumpanakis, P., 1993. Turbulence modeling of flow in axisymmetric rotor–stator systems. *Proc. 5th Int. Symposium on Refined Flow Modeling and Turbulence Measurements*, IAHR, Paris, France

Ito, H. and Nanbu, K. 1971. Flow in rotating straight pipes of circular cross-section. *J. Basic Eng.*, **93**, 383

Itoh, M., Yamada, Y., Imao, S. and Conda, M. 1990. Experiments on turbulent flow due to an enclosed rotating disk. *Proc. 1st Symposium on Engineering Turbulence Modeling and Measurement* (659–668), Elsevier, New York

Kays, W. M. and Moffat, R. J. 1975. The behavior of transpired turbulent boundary layers. In *Studies in Convection — 1*, Academic, Orlando, FL, 223–319

Khodak, A. E., Kirillov, A. I., Ris, V. V. and Smirnov, E. M. 1992. Numerical simulation of secondary flows and longitudinal roll-ceil structures in rotating channels. *Comp. Fluid Dynamics*, **2**, 597–604

Kilic, M., Gan, X. and Owen, J. M., 1994. Turbulent flow between two discs contrarotating at differential speeds. *Proc. Int Gas-Turb. and Aero Congress* (ASME Paper 94-GT-54), The Hague, The Netherlands

Launder, B. E. and Li, S. P. 1994. On the elimination of wall-topography parameters from second-moment closure. *Phys. Fluids*, **6**, 999–1006

Launder, B. E., Reece, G. J. and Rodi, W. 1975. Progress in the development of a Reynolds-stress turbulence closure. *J. Fluid Mech.*, **68**, 537–566

Launder, B. E. and Sharma, B. I. 1974. Application of the energy dissipation model of turbulence to the calculation of flow near a spinning disc. *Lett. Heat Mass Transfer*, **1**, 131–138

Li, H- Y. 1995. Ph. D. Thesis, Department of Mechanical Engineering, Faculty of Technology, UMIST, Manchester, UK

Lien, F. S. 1993. Contribution to round normally impinging turbulent jet and turbulent flow through tube bank sub-channel. *Proc. 2nd ER-COFTAC-IAHR Workshop on Refined Flow Modelling* M. A. Leschziner and B. E. Launder (eds.), (p. 68), Manchester, UK

Liou, T- M., Huang, J- J. and Chen, S- S. 1993. Simulation and measurements of enhanced turbulent heat transfer in a channel with periodic ribs on one principal wall. *Int. J. Heat Mass Transfer*, **36**, 507–517

Long, C., Morse, A. P. and Zafiropoulos, N. 1993. Buoyancy-affected flow and heat transfer in asymmetrically heated rotating cavities, *Proc. Int. Gas-Turb. and Aero Congress* (ASME Paper 93-GT-88), Cincinnati, OH, USA

Louis, J. F. and Salhi, A. 1988. Turbulent flow velocity between rotating co-axial disks of finite radius. *Proc. Int. Gas-Turb. and Aero Congress* (ASME Paper 88-GT-47), Amsterdam, The Netherlands

Majumdar, A. K., Pratap, V. S. and Spalding, D. B. 1977. Numerical computation of flow in rotating ducts. *J. Fluids Eng.*, **99**, 148–153

Majumdar, A. K. and Spalding, D. B. 1977. A numerical investigation of three-dimensional flows in a rotating duct by a partially parabolic procedure. ASME Paper 77-WA/FE-7

Morse, A. P. 1988. Numerical prediction of turbulent flow in rotating cavities. *J. Turbomachinery*, **110**, 202–212

Morse, A. P. 1991a. Application of a low-Reynolds number k-ε turbulence model to high-speed rotating cavity flows. *J. Turbomachinery*, **113**, 98–105

Morse, A. P. 1991b. Assessment of laminar-turbulent transition in closed disk geometries. *J. Turbomachinery*, **113**, 131–138

Morse, A. P. and Ong, C. L. 1992. Computation of heat transfer in rotating cavities, using a two-equation model of turbulence. *J. Turbomachinery*, **114**, 247–255

Nikas, K. 1995. M. Sc. Dissertation, Department of Mechanical Engineering, UMIST, Manchester, UK

Prakash, C. and Zerkle, R. 1992. Prediction of turbulent flow and heat transfer in a radially rotating square duct. *J. Turbomachinery*, **114**, 835–845

Rodi, W. 1976. A new algebraic stress relation for calculating the reynolds stresses. *Z. Ang. Math. Mech* (ZAMM), **56**, 219

Sathyamurthy, P. S., Karki, K. C. and Patankar, S. V. 1994. Prediction of turbulent flow and heat transfer in a rotating square duct with 180° bend, *Proc. Int. Gas-Turb. and Aero Congress* (ASME Paper 94-GT-197), The Hague, The Netherlands

Schiestel, R., Elena, L. and Rezoug, T. 1993. Numerical modeling of turbulent flow and heat transfer in rotating cavities. *Num. Heat Trans. A*, **24**, 45–65

Shah, J. D. 1971. Prediction of flow and heat transfer over rough elements. M. Sc. Thesis, Imperial College, London University, London, UK

Sturgess, H. J. and Dalla, P. 1987. Calculation of flow development in rotating passages for cooled gas turbine blades. *Proc. ASME Int. Comp. and Engineering Conference and Exhibition*, New York, NY, USA

Taylor, C., Rance, C. and Medwell, J. O. 1985. A method for the prediction of Coriolis induced secondary flows and their influence on heat transfer in rotating ducts. *Eng. Comp.* **2**, 2–12.

Taylor, C., Xia, J. Y., Medwell, J. O. and Morris, W. D. 1991. Numerical representation of heat transfer into turbine blade cooling ducts, *Proc. 77th Symposium Propulsion Applications* (AGARD CD510, PEP), San Antonio, Texas, USA

Te Braak, M. A. F. 1994. Low-Reynolds number turbulence modeling in rotating disc cavities. Ph. D. thesis, Vakgroep Thermische Werkluigbouwkunde, Faculteit der Werktuigbouwkunde, Universiteit Twente, Twente, The Netherlands

Tolpadi, A. K. 1994. Calculation of heat-transfer in a radially rotating coolant passage. *Num. Heat Transfer, A* **26**, 683–700

Ton, F. K. and Lin, C. A. 1994. Predictions of turbulent flows between a rotating and a stationary disk, *Proc. Symposium on Turbulent Heat and Mass Transfer*, Lisbon, Portugal

Van Driest, E. R., 1956. On turbulent flow near a wall. *J. Aero, Soc.*, **23**, 1007

Virr, G. P., Chew, J. W. and Coupland, J. 1993. Application of computational fluid dynamics to turbine disc cavities, *Proc. Int. Gas-Turb. and Aero Congress*, Cincinnati, OH, USA

Wagner, J. H., Johnson, B. V. and Hajek, T. J. 1989 Heat transfer in rotating passages with smooth walls. *Proc. Int. Gas-Turb. and Aero Congress* (ASME Paper 89-GT-272)

Xia, J. Y. and Taylor, C. 1993. The prediction of turbulent flow and heat transfer in a tight square sectioned 180° bend. *Proc. 8th Int. Conference on Numerical Methods in Laminar and Turbulent Flow*, Swansea, Wales

Younis, B. A. 1993. Prediction of turbulent flows in rotating rectangular ducts. *J. Fluids Eng.*, **115**, 646–652

Zhou, H. and Leschziner, M. A. 1988. A local oscillation-damping algorithm for higher-order convection schemes. *Comp. Meth. Appl. Mech. Eng.*.